

# Hydrogen storage in carbon nanotubes and related materials

Gautam Gundiah,<sup>a</sup> A. Govindaraj,<sup>a</sup> N. Rajalakshmi,<sup>b</sup> K. S. Dhathathreyan<sup>b</sup> and C. N. R. Rao<sup>\*a</sup>

<sup>a</sup>Chemistry and Physics of Materials Unit and CSIR Centre of Excellence in Chemistry, Jawaharlal Nehru Centre for Advanced Scientific Research, Jakkur P. O., Bangalore 560 064, India. E-mail: cnrrao@jncasr.ac.in

<sup>b</sup>Centre for Energy Research, SPIC Science Foundation, 64 Mount Road, Guindy, Chennai 600 032, India

Received 19th July 2002, Accepted 7th November 2002

First published as an Advance Article on the web 28th November 2002

Adsorption of hydrogen at 300 K has been investigated on well-characterized samples of carbon nanotubes, besides carbon fibres by taking care to avoid many of the pitfalls generally encountered in such measurements. The nanotube samples include single- and multi-walled nanotubes prepared by different methods, as well as aligned bundles of multi-walled nanotubes. The effect of acid treatment of the nanotubes has been examined. A maximum adsorption of *ca.* 3.7 wt% is found with aligned multi-walled nanotubes. Electrochemical hydrogen storage measurements have also been carried out on the nanotube samples and the results are similar to those found by gas adsorption measurements.

## Introduction

The early report of Dillon *et al.*<sup>1</sup> that carbon nanotubes can be used to store considerable amounts of hydrogen created high expectations.<sup>2</sup> Dillon *et al.* used unpurified soot containing 0.1–0.2 wt% of single-walled carbon nanotubes (SWNTs) and obtained 0.01 wt% of H<sub>2</sub> storage at 0 °C. They extrapolated that SWNTs had 5 wt% H<sub>2</sub> storage capacity assuming that only the nanotubes were responsible for the H<sub>2</sub> uptake. Since then, several workers have examined H<sub>2</sub> adsorption with carbon fibres as well as nanotubes produced by different methods.<sup>3–7</sup> While Liu *et al.*<sup>8</sup> reported a H<sub>2</sub> storage capacity of 4.2 wt% in SWNTs generated by a semicontinuous hydrogen arc-discharge method, Ye *et al.*<sup>9</sup> found a gravimetric H<sub>2</sub> storage capacity as high as 8.25 wt% in high purity cut-SWNTs at 80 K under a pressure of *ca.* 7 MPa. Chen *et al.*<sup>10</sup> have reported a hydrogen storage capacity upto 13 wt% with aligned multi-walled carbon nanotubes (MWNTs). These workers employed quadrupole mass spectrometry and thermogravimetric analysis to study H<sub>2</sub> desorption properties. Interesting results on hydrogen storage have been reported with alkali-doped carbon nanotubes.<sup>11</sup> Li- and K-doped carbon nanotubes are reported to adsorb 20 and 14 wt% of H<sub>2</sub>, respectively, at 1 atm. pressure, at 200–400 °C in the case of Li-doped nanotubes and near room temperature for the K-doped nanotubes. A lower, but substantial, H<sub>2</sub> adsorption was also reported for alkali-doped graphite. The highest capacity for H<sub>2</sub> storage (up to 67%) reported to date is that by Chambers *et al.*<sup>12</sup> for graphite nanofibres at ambient temperatures and at a pressure of 11.35 MPa. Electrochemical hydrogen storage in carbon nanotube materials was carried out by Nützenadel *et al.*<sup>13</sup> on as-prepared SWNTs and MWNTs. For the SWNT samples, the measured discharge capacities indicated a storage capacity of 0.39 wt% (110 mA h g<sup>-1</sup>). SWNTs are also reported to show reversible charging capacities of up to 800 mA h g<sup>-1</sup> corresponding to a capacity of 2.9 wt%.<sup>14</sup>

In spite of several of the favorable reports listed above, the scenario is not encouraging. Some of the recent papers report hardly any adsorption in the different carbon nanostructures, the maximum adsorption in some cases being lower than 1 wt%.<sup>15,16</sup> In view of the importance of the subject and also the wide differences amongst the various findings, we considered it

important to carry out H<sub>2</sub> adsorption measurements systematically on well-characterized samples of carbon nanotubes and fibres prepared by different methods. We have, therefore, carried out measurements on SWNTs produced by the arc-discharge method, on MWNTs synthesized by arc-discharge and by the pyrolysis of acetylene over catalysts, on aligned multi-walled nanotubes obtained by the pyrolysis of organometallic precursors as well as carbon fibres. The measurements have been carried out on as-synthesized samples as well as samples subjected to acid treatment to remove catalyst particles. In addition to carrying out adsorption measurements, we have performed electrochemical studies of hydrogen storage on these materials.

## Experimental

The carbon samples that we studied for hydrogen storage are as follows: SWNTs synthesized by the arc-discharge method (as-synthesized), **I**; SWNTs synthesized by the arc-discharge method (treated with conc. HNO<sub>3</sub>), **II**; MWNTs synthesized by the pyrolysis of acetylene (as-synthesized), **III**; MWNTs synthesized by the pyrolysis of acetylene (treated with conc. HNO<sub>3</sub>), **IV**; MWNTs synthesized by the arc-discharge method, **V**; aligned MWNT bundles synthesized by the pyrolysis of ferrocene (as-synthesized), **VI**; aligned MWNT bundles synthesized by the pyrolysis of ferrocene (treated with acid), **VII**; aligned MWNT bundles synthesized by the pyrolysis of ferrocene and acetylene (as-synthesized), **VIII**; and aligned MWNT bundles synthesized by the pyrolysis of ferrocene and acetylene (treated with acid), **IX**.

Scanning electron microscopy (SEM) images for all the samples were obtained on a LEICA S440i scanning electron microscope. Transmission electron microscopy (TEM) images were obtained with a JEOL JEM 3010 operating with an accelerating voltage of 300 kV. In order to find out the percentage of catalyst particles, thermogravimetric analysis (TGA) was performed on the samples.

SWNTs, **I**, were produced by the dc arc-discharge method using a composite graphite rod containing Y<sub>2</sub>O<sub>3</sub> (1 at%) and Ni (4.2 at%) as anode and a graphite rod as cathode under a helium pressure of 660 Torr with a current of 100 A and 30 V as

reported earlier.<sup>17</sup> The web-like product obtained was heated at 300 °C in air for *ca.* 24 h to remove amorphous carbonaceous materials. In order to remove the catalyst particles and open the ends of the nanotubes, the sample was stirred with concentrated nitric acid at 60 °C for *ca.* 12 h and washed with distilled water in order to remove the dissolved metal particles.<sup>18</sup> We denote the acid-treated SWNTs as **II**. The SWNTs in **I** had bundles of 5–50 nanotubes as revealed by high-resolution electron microscopy (HREM). The diameter of the nanotubes is in the range 1.2–1.4 nm. We show a typical HREM image of sample **II** in Fig. 1(a). There is a negligible amount of amorphous carbon and of metal particles adhering to the nanotubes.

MWNTs, **III**, were prepared by the decomposition of acetylene at a flow rate of 50 standard cubic centimeters per minute (sccm) at 730 °C over an iron/silica catalyst in flowing hydrogen (75 sccm) according to a previously reported method.<sup>19</sup> The silica was removed by treatment with aqueous hydrofluoric acid (HF) for 12 h. The metal catalyst particles in **III** were removed by treatment with concentrated nitric acid at 60 °C for *ca.* 12 h and washing with distilled water. The acid-treated sample was heated at 350 °C to obtain **IV**. Nanotubes **III** had diameters of between 25 and 75 nm with lengths up to tens of microns [Fig. 1(b)]. The TEM images, however, showed the presence of extraneous carbonaceous material and catalyst particles. HREM images showed that they were not very well graphitized, presumably due to the low temperatures at which they were prepared. Upon treatment with conc. HNO<sub>3</sub>, we found that we were able to remove a majority of the catalyst particles, which was also verified by TGA. Furthermore, the nanotubes had open ends as revealed by TEM images.

MWNTs were also prepared by striking an arc between graphite electrodes in 500 Torr of helium by a previously published method.<sup>20</sup> A current of 60–100 A across a potential drop of *ca.* 25 V gives high yields of carbon nanotubes. The nanotubes thus obtained were opened by heating to 600 °C in air. This sample, denoted by **V**, had nanotubes with diameters in the 300 nm range with lengths of several microns. They had open ends but were well graphitized as revealed by the HREM images.

Aligned bundles of MWNTs, **VI**, were synthesized by the pyrolysis of ferrocene in an Ar atmosphere by a previously reported method.<sup>20</sup> The sample was scraped out from the walls of the quartz tube. We show an SEM image of the aligned MWNTs, **VI**, in Fig. 1(c). The nanotubes are well aligned with lengths extending to tens of microns. In order to remove the catalyst particles, a sample of **VI** was treated with concentrated nitric acid for 4 h, followed by washing thoroughly with distilled water and drying. This acid-treated sample, denoted

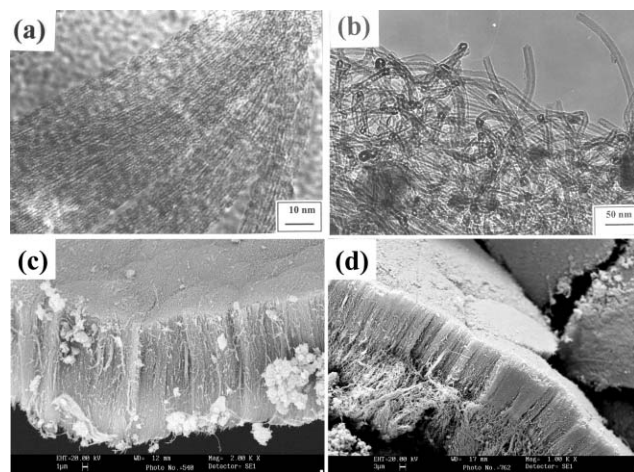


**Fig. 1** (a) HREM image of **II**, (b) low magnification TEM image of **III**, (c) SEM image of **VI**, and (d) SEM image of **VIII**.

by **VII**, had open ends, but the alignment was retained. In order to synthesize dense bundles of aligned nanotubes (**VIII**), a mixture of acetylene (85 sccm) and ferrocene was sublimed. In Fig. 1(d) we show an SEM image of this sample. The catalyst particles in **VIII** were removed by treating the aligned bundles with conc. nitric acid for 4 h and then washing thoroughly with distilled water. The acid-treated sample, **IX**, was dried at 100 °C.

Carbon fibres were synthesized by the decomposition of acetylene at a flow rate of 20 sccm at 750 °C over a nickel/silica catalyst in flowing argon (80 sccm). The silica was removed by treatment with aqueous HF for 12 h. We show a low magnification SEM image of the carbon fibres prepared by us in Fig. 2(a). The yield of the fibres was good, with the fibres having diameters of *ca.* 200 nm and lengths up to 1 μm. The HREM image of this sample in Fig. 2(b) shows that the fibres are not well graphitized, with the planes inclined at an angle of *ca.* 32° with respect to the fibre axis.

In order to decorate the MNWTs with Pd and Pt nanoparticles, the nanotubes prepared by the pyrolysis route, **III**, were treated with conc. HNO<sub>3</sub> in order to remove the metal catalyst and then washed repeatedly with distilled water and dried at 100 °C. The decoration by Pt and Pd was carried out by reduction of the appropriate metal compound, namely H<sub>2</sub>PtCl<sub>4</sub> and H<sub>2</sub>PdCl<sub>6</sub>, respectively, by employing the appropriate reducing agent.

The apparatus used for hydrogen adsorption experiments was custom-built and similar to that described elsewhere.<sup>12</sup> It consisted of a high-pressure stainless steel sample cell that was connected to a high-pressure reservoir *via* a high-pressure bellows valve. The pressure was monitored using a pressure gauge that was connected in the system. Experiments were conducted to verify that the system was leak-free. This was done by pressurizing the unit, and verifying that the pressure remained constant over a period of 10 h. Calibration of the system to account for the pressure drop brought about by the increase in volume upon opening of the valve between the reservoir and the evacuated sample cell at various pressures was also carried out. The volume of gas contained in the system at various pressures in the absence of the carbon samples was determined by allowing it to exit the system and then measuring by the displacement of water.

Hydrogen adsorption experiments were performed at 300 K. The hydrogen that was used was of ultra high purity

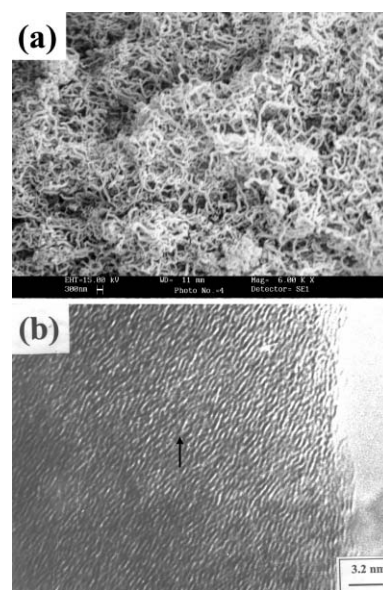


**Fig. 2** (a) SEM image of as-synthesized carbon fibres; (b) HREM image of carbon fibres showing the stacking of graphitic planes. The arrow denotes the direction of growth of the fibre.

(>99.99%), with an impurity (e.g. moisture and nitrogen) content of less than 10 ppm. The carbon samples were accurately weighed and taken in the sample cell. The sample cell was evacuated to  $10^{-5}$  Torr and heated for 12 h at 125 °C in order to degas the sample. This vacuum is sufficient as per the IUPAC recommendations on adsorption measurements.<sup>21</sup> Hydrogen was then introduced into the reservoir container and subsequently let into the sample cell. The drop in pressure from the initial value, of ca. 145 bar, was measured at regular intervals. The amount of hydrogen stored in the samples was calculated from the changes in pressure following the interaction of the material with the gas. Blank tests were repeated at regular intervals to verify that the system was free of leaks and that the pressure drop observed was only due to the uptake of hydrogen by the samples. The weight of the sample was 125 mg or more, to minimize errors in measurements. All of the adsorbed hydrogen could be desorbed, as established by adsorption–desorption experiments, the only desorbed gas being hydrogen.

Electrochemical measurements were carried out using an EG&G galvanostat/potentiostat model 273, with the help of a three electrode system using the samples as the working electrode, platinum as the counter electrode and saturated calomel as the reference electrode. Electrochemical measurements were carried out in a flooded electrolyte condition in open cells. The electrolyte, 30% KOH, which is the same as that used in alkaline batteries, was prepared from reagent grade KOH and de-ionized water. Chronopotentiometry, controlled potential coulometry, and cyclic voltammetry were used. Electrodes were prepared by mixing 10 mg of the nanotube samples with Cu powder in the ratio of 1:3 with a polytetrafluoroethylene (PTFE) binder. The putty form of the mixture was mechanically pressed on to a current collector (Ni mesh) at room temperature. Then the electrode was sintered at 200 °C for about 1 h under vacuum. The geometric area of the electrode was ca. 2 cm<sup>2</sup>. The electrodes were tested for their charge–discharge characteristics, initial capacity and cycle life.

## Results and discussion

### H<sub>2</sub> adsorption

Unlike metal alloys that adsorb hydrogen after a short period of incubation, hydrogen is adsorbed soon after it is admitted in the carbon samples studied by us. The entire adsorption was over within 100–150 min. Similar observations have been made by other workers.<sup>8,12</sup>

In Fig. 3, we show plots of hydrogen adsorption *versus* time

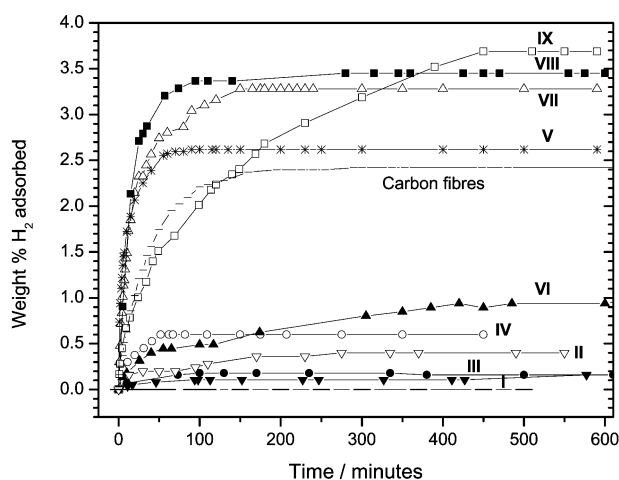


**Fig. 3** Amount of hydrogen adsorbed in wt% as a function of time for the various carbon nanostructures. The broken curve represents the blank data obtained in the absence of a carbon sample.

for the various carbon nanostructured samples studied by us. The broken curve representing the blank run with an adsorption of 0.0 wt% was obtained when the system was evacuated and then pressurized with hydrogen gas in the absence of a carbon sample. This indicates that there is no adsorption by the system itself in the absence of the carbon sample. Similar blank runs, performed after each adsorption experiment with a carbon sample, showed identical curves. The SWNT sample **I** showed a storage capacity of 0.2 wt%. On removal of the catalyst particles, the storage capacity for the sample **(II)** increased only slightly to 0.4 wt%. This indicates that the catalyst particles are probably inert with regard to H<sub>2</sub> adsorption. The H<sub>2</sub> storage that we have obtained for SWNTs is considerably lower than that reported by others.<sup>1,8</sup> We further cleaned the surface of the tubes by treatment with a mixture of conc. HCl and H<sub>2</sub>O<sub>2</sub> and were able to obtain a storage capacity of 1.2 wt%. This treatment would remove any extra carbonaceous materials that may block the pores and hinder the entry of the hydrogen molecules, as evidenced by the HREM images (not shown).

The hydrogen storage capacity for the MWNT sample **III** was 0.2 wt% as shown in Fig. 3. These results are consistent with the values obtained by Cao *et al.*<sup>22</sup> who obtained low H<sub>2</sub> storage for random MWNTs. Opening of the tubes **(IV)** increased the hydrogen storage capacity to 0.6 wt% (Fig. 3). The low values for adsorption may be due to the fact that the nanotubes are not well graphitized since the temperatures we used in their synthesis were low. Well-graphitized MWNTs have been reported to show higher percentages of hydrogen adsorption.<sup>23</sup>

We find the MWNTs, **V**, which were well graphitized, show an increased hydrogen storage capacity of 2.6 wt% as shown in Fig. 3. It appears that opened nanotubes show slightly higher storage as shown by samples **IV** and **V**.

The hydrogen storage capacity for sample **VI** is 1.0 wt%, which is considerably higher than that shown for the random MWNTs prepared by the pyrolysis route. This value is considerably less than that reported by Chen *et al.*<sup>10</sup> who studied the desorption of hydrogen using thermogravimetric analysis and reported a value of 5–7 wt% at around 10 atm. The present value is to be compared to that of Cao *et al.*<sup>22</sup> who reported a hydrogen storage of 2.4 wt% at slightly lower pressures of around 100 bar. Hydrogen is expected to be stored between the graphite layers as well as in the pores formed by the inter-nanotube space between adjacent parallel nanotubes.<sup>10,22</sup> We expect that if the catalyst can be removed, hydrogen would also be stored in the hollow center of the tubes, which is the storage mechanism for SWNTs.<sup>1,8</sup> Accordingly, we could reproducibly achieve a H<sub>2</sub> storage capacity of 3.3 wt% for sample **VII**, as shown in Fig. 3. On increasing the packing density of the aligned nanotubes (sample **VIII**), we found only a marginal increase in the storage capacity (Fig. 3), the value being 3.5 wt%. On acid treatment and removal of metal particles, the sample, **IX**, showed even a higher storage capacity of 3.7 wt%. This is the highest storage capacity obtained by us in the present study.

In order to ensure the validity of the results in Fig. 3, we carried out independent adsorption experiments at different pressures of hydrogen. At first, measurements were performed at a high pressure followed by desorption at 300 °C in a vacuum ( $10^{-5}$  Torr) and re-adsorption at a lower pressure. We show the results of such studies on sample **IX** in Fig. 4, where the wt% of H<sub>2</sub> (after desorption and re-adsorption) is plotted against pressure. The results show the expected trend with a decrease in storage with any decrease in pressure.

The adsorption curve for the carbon fibres is also shown in Fig. 3. We see that the storage is 2.4 wt%, higher than in some of the nanotube samples, but lower than the 3.7 wt% storage found with **IX**. It appears that hydrogen is between graphite planes of the fibres.<sup>12</sup> The storage capacity found by us is

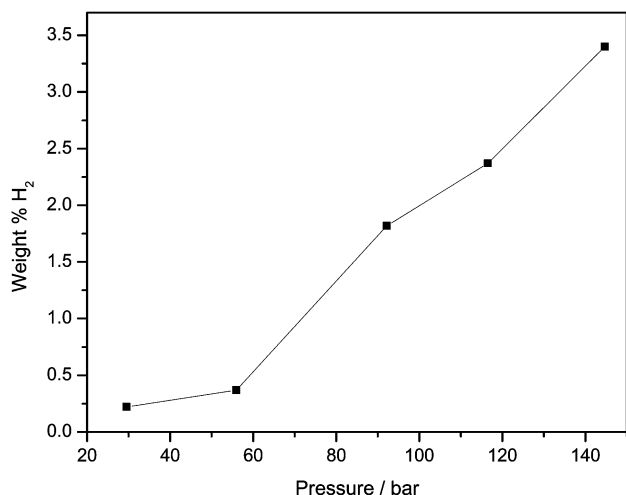


Fig. 4 Hydrogen storage in aligned MWNTs (acid-treated), sample IX, at different pressures.

considerably lower than that reported in the literature.<sup>12,24</sup> The low storage capacity may partly be due to incomplete crystallization. Furthermore, the fibres do not distinctly have a herringbone structure present in the samples employed by Chambers *et al.*<sup>12</sup> In order to remove the catalyst particles from the fibres, we treated the sample with conc. HNO<sub>3</sub> but found that the morphology was disrupted badly, resulting in a very low storage capacity (0.8 wt%).

It has been pointed out by Tibbetts *et al.*<sup>16</sup> that erroneous H<sub>2</sub> adsorption data can result from the small sample weights. We therefore performed adsorption studies using different weights of VII. The results of the adsorption are shown in Fig. 5. Thus, with sample weights of 138.5 and 200 mg, the shape of the adsorption curve remained the same as did the storage capacity (3.3 wt%).

### Electrochemical measurements

The mechanism of electrochemical storage is different from gaseous storage in that with electrochemical storage the nanotubes behave like metal hydride electrodes in Ni-MH batteries. In metal hydride batteries, hydrogen is stored reversibly in the interstitial sites of a host metal and electric energy is produced by direct electrochemical conversion.<sup>25,26</sup> In the gaseous storage, however, the process is pure physisorption.

We carried out electrochemical measurements of hydrogen storage on the various nanotube samples as well as on the carbon fibres. In addition, we carried out measurements on

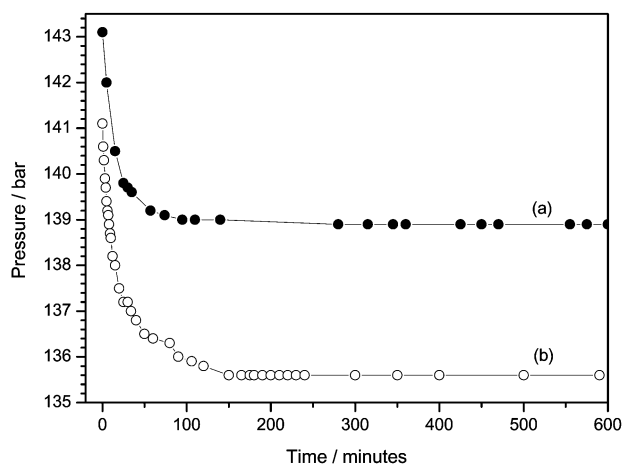


Fig. 5 Plots of pressure versus time for the MWNT bundles, VII, obtained with (a) 138.5 mg, and (b) 200 mg of the sample.

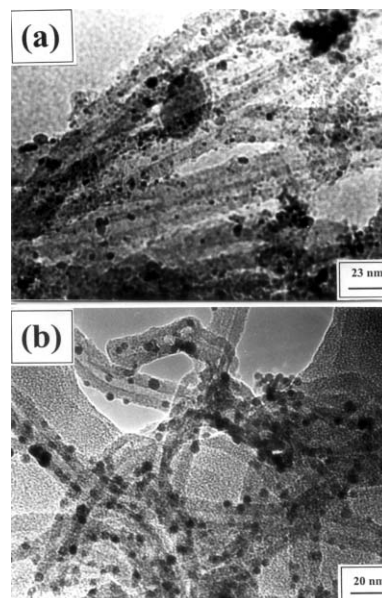


Fig. 6 Low magnification TEM images of (a) Pt-decorated MWNTs, and (b) Pd-decorated MWNTs.

MWNTs decorated with Pt and Pd nanoparticles. In Fig. 6(a), we show a low magnification TEM image of the Pt-decorated MWNTs. The size of the Pt nanoparticles is below 5 nm, while the nanotubes have diameters of *ca.* 35 nm. Thermogravimetric analysis revealed the loading of Pt in the sample to be 1.8%. We show a low magnification TEM image of the Pd-decorated nanotubes in Fig. 6(b). The Pd nanoparticles have a diameter of around 5 nm and the MWNTs have diameters of *ca.* 25 nm. The loading of Pd in the sample was 4.1%, as shown by TGA. An examination of the metal-decorated nanotubes suggests that the metal nanoparticles get deposited on the acid sites, which are dispersed all over the surface of the nanotubes.

The charging capacities of the various samples are shown in Fig. 7. Also shown are the corresponding weight percentages of hydrogen stored. The best result was obtained with sample VIII which showed a charging capacity of 1050 mA h g<sup>-1</sup> (3.7 wt%). The hydrogen storage capacities obtained by gas adsorption and by the electrochemical method are comparable.

It is seen that the electrochemical charging capacity initially increases with the cycle. It reaches saturation after some cycles and then becomes stabilized. With most of the samples studied,

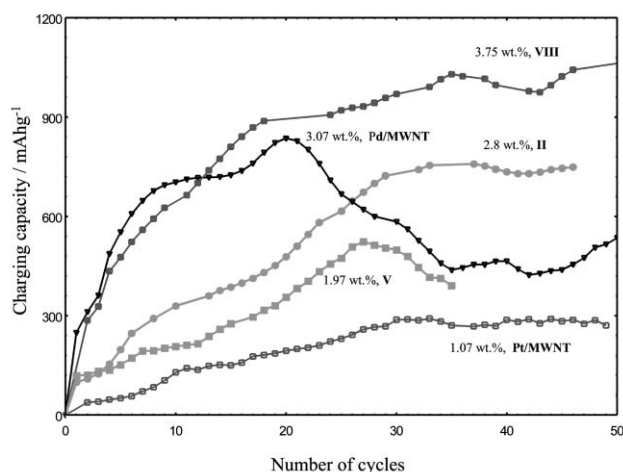


Fig. 7 Plot of the charging capacity against the number of cycles for different carbon nanostructures. Also shown are the corresponding weight percentages of H<sub>2</sub> stored.

the electrode was stable even after 50 cycles. In the case of Pd-loaded MNWTs, the cyclic stability was not good, as there was the degradation of the electrode after 20 cycles with the charging capacity decreasing from 800 to 200 mA h g<sup>-1</sup>. Sample V, the arc-discharge MWNTs, also seems to have a poor cyclic stability. But the advantage of these samples is that the maximum capacity is obtained at a lower cycle number (around 20), compared with other samples, where the maximum capacity is obtained only after 30 cycles. This shows that the kinetics of hydrogen absorption are fast in these systems.

## Conclusions

The maximum H<sub>2</sub> storage capacity achieved by us is obtained with densely aligned bundles of MNWTs that have been treated with acid. We find that carbon fibres do not show the exceptional storage capacities reported by others. Though the maximum capacity we have achieved in our studies with the nanotubes is 3.7 wt%, we are well below the 6.5 wt% benchmark set by the US Department of Energy (DOE). We have verified that the results obtained by us are reproducible as confirmed by experiments at lower pressures and with different weights of samples. The hydrogen storage in the samples has been studied electrochemically to obtain values that are similar to the gas storage values.

Though there have been a few recent reports of very low percentages of hydrogen storage in carbon nanotubes,<sup>15,16</sup> there have also been reports giving detailed procedures for the synthesis and purification along with good H<sub>2</sub> storage capacities.<sup>22,23</sup> What is noteworthy in the present study is that we have avoided many of the pitfalls by using different sample weights as well as by doing experiments at lower pressures. It is also significant that the hydrogen storage capacities obtained by the gas adsorption method are similar to those obtained electrochemically.

## Acknowledgement

The authors thank the Department of Science and Technology, Government of India, for support of this research.

## References

- 1 A. C. Dillon, K. M. Jones, T. A. Bekkedahl, C. H. Kiang, D. S. Bethune and M. J. Heben, *Nature*, 1997, **386**, 377.

- 2 C. Zandonella, *Nature*, 2001, **410**, 734.
- 3 R. G. Ding, G. Q. Lu, Z. F. Yan and M. A. Wilson, *J. Nanosci. Nanotechnol.*, 2001, **1**, 7.
- 4 H. M. Cheng, Q. H. Yang and C. Liu, *Carbon*, 2001, **39**, 1447.
- 5 M. S. Dresselhaus, K. A. Williams and P. C. Eklund, *MRS Bull.*, 1999, **24**, 45.
- 6 J. E. Fischer, *Chem. Innov.*, 2000, **30**, 21.
- 7 A. C. Dillon and M. J. Heben, *Appl. Phys. A*, 2001, **72**, 133.
- 8 C. Liu, Y. Y. Fan, M. Liu, H. T. Cong, H. M. Cheng and M. S. Dresselhaus, *Science*, 1999, **286**, 1127.
- 9 Y. Ye, C. C. Ahn, C. Witham, B. Fultz, J. Lui, A. G. Rinzler, D. Colbert, K. A. Smith and R. E. Smalley, *Appl. Phys. Lett.*, 1999, **74**, 2307.
- 10 Y. Chen, D. T. Shaw, X. D. Bai, E. G. Wang, C. Lund, W. M. Lu and D. D. L. Chung, *Appl. Phys. Lett.*, 2001, **78**, 2128.
- 11 P. Chen, X. Wu, J. Lin and K. L. Tan, *Science*, 1999, **285**, 91.
- 12 A. Chambers, C. Park, R. T. K. Baker and N. M. Rodriguez, *J. Phys. Chem. B*, 1998, **102**, 4253.
- 13 C. Nützenadel, A. Züttel, D. Chartouni and L. Schlapbach, *Electrochem. Solid State Lett.*, 1999, **2**, 30.
- 14 N. Rajalakshmi, K. S. Dhathathreyan, A. Govindaraj and B. C. Satishkumar, *Electrochem. Acta*, 2000, **45**, 4511.
- 15 M. Ritschel, M. Uhlemann, O. Gutfleisch, A. Leonhardt, A. Graff, Ch. Täschner and J. Fink, *Appl. Phys. Lett.*, 2002, **80**, 2985.
- 16 G. G. Tibbetts, G. P. Meisner and C. H. Olk, *Carbon*, 2001, **39**, 2291.
- 17 C. Journet, W. K. Maser, P. Bernier, A. Loiseau, M. Lamy de la Chapelle, S. Lefrabt, P. Denierd, R. Lee and J. E. Fischer, *Nature*, 1997, **388**, 756.
- 18 C. N. R. Rao, A. Govindaraj, R. Sen and B. C. Satishkumar, *Mater. Res. Innov.*, 1998, **2**, 128.
- 19 K. Hernadi, A. Fonseca, J. B. Nagy, D. Bernaerts, J. Riga and A. Lucas, *Synth. Met.*, 1996, **77**, 31.
- 20 R. Seshadri, A. Govindaraj, H. N. Aiyer, R. Sen, G. N. Subbanna, A. R. Raju and C. N. R. Rao, *Curr. Sci. (India)*, 1994, **66**, 839; C. N. R. Rao, R. Sen, B. C. Satishkumar and A. Govindaraj, *Chem. Commun.*, 1998, 1525.
- 21 K. S. W. Sing, D. H. Everett, R. A. W. Haul, L. Moscou, R. A. Pierotti, J. Rouquérol and T. Siemieniowska, *Pure Appl. Chem.*, 1985, **57**, 603.
- 22 A. Cao, H. Zhu, X. Zhang, X. Li, D. Ruan, C. Xu, B. Wei, J. Liang and D. Wu, *Chem. Phys. Lett.*, 2001, **342**, 510.
- 23 P. X. Hou, Q. H. Yang, S. Bai, S. T. Xu, M. Liu and H. M. Cheng, *J. Phys. Chem. B*, 2002, **106**, 963.
- 24 Y. Y. Fan, B. Liao, M. Liu, Y. L. Wei, M. Q. Lu and H. M. Cheng, *Carbon*, 1999, **37**, 1649.
- 25 J. M. Evjen and A. J. Catotti, in *Handbook of Batteries*, D. Linden, ed., McGraw-Hill, New York, 2nd edn., 1995, ch. 27.
- 26 M. A. Fetcenko and S. Venkatesan, *Prog. Batteries Sol. Cells*, 1990, **9**, 259.